Available online at www.sciencedirect.com
SCIENCE DIRECT®
Journal of Nuclear Materials 329–333 (2004) 1003–1007
journal of nuclear materials
www.elsevier.com/locate/jnucmat

Helium effects on EUROFER97 martensitic steel irradiated by dual-beam from 1 to 50 dpa at 250 and 300 °C with 10 He appm/dpa

Gang Yu [a], Xiaoqiang Li [a], Jinnan Yu [a,*], Yican Wu [b], H. Kinoshita [c], H. Takahashi [c], M. Victoria [d]

[a] China Institute of Atomic Energy, P.O. Box 275-51, Beijing 102413, PR China
[b] Institute of Plasma Physics, P.O. Box 1126, Hefei 230031, PR China
[c] CARET, Hokkaido University, Kita-13 Nishi-8, Kita-ku, Sapporo 060-8628, Japan
[d] CRPP–EPFL Fusion Technology Materials, 5232 Villigen PSI, Switzerland

Abstract

Reduced activation martensitic steel specimens were irradiated by dual-beam from 0.1 to 50 dpa at 250 and 300 °C with 10 He appm/dpa. The in-situ microstructure observation shows that the bubbles were present after 1.7 dpa for 250 °C irradiation and after 0.1 dpa for 300 °C irradiation. The bubble size distribution is a Maxwell distribution, which evolves to a bimodal distribution with increasing damage dose. The transition occurs after 10 dpa at 300 °C irradiation and after 30 dpa at 250 °C irradiation. The bubble concentration and peak bubble size are similar for various doses at 250 °C, and are 3.8×10^{21} m^{-3} and 2.5 nm, respectively. The size of cavities at the second peak of the bimodal distribution is around 6 nm. The cavity size distribution increases and spreads out with damage dose increase. The dislocation loops are typical interstitial dislocation loops that evolve from black–white spots to visible interstitial loops. The size range of interstitial loops is between 2.5 and 11 nm and the dislocation loop density increases monotonically with the damage dose.

1. Introduction

Fusion reactor technology and materials study is an important part of fusion energy development program. Austenitic stainless steels have been selected as First Wall (FW) and blanket (B) structure material. Limitations from swelling, inferior thermal properties, helium embrittlement, compatibility with liquid metal (Pb–Li, Li, etc.) above 400 °C [1] and microstructure instability forced investigators to explore other materials. The martensitic steels suffer less from these phenomena than the austenitic steels. Their compatibility with liquid metal (Pb–Li, Li) is hold up to 480 °C and they can be made in reduced activation compositions. The reduced activation martensitic (RAM) steel is presently the most realistic contender for application in fusion blankets (as FW/B structure materials) near the magnetically confined plasma [2–5]. A concept, such as the helium-cooled pebble bed (HCPB) and the water-cooled lithium-lead (WCLL) blankets, to be tested integrally in ITER or its successor, has been designed with RAFM steel [6].

The serious issue is loss of fracture toughness (associated with a DBTT shift) by irradiation at low temperature [7]. Because the effect of irradiation on DBTT is rather small at temperature higher than 400 °C [8], the irradiation induced DBTT shift may not be a problem for the gas or liquid metal cooled blanket concept operated above 400 °C. But the use of martensitic steels in the Steady State Tokamak Reactor (SSTR) designed

* Corresponding author. Tel.: +86-10 693 572 32; fax: +86-10 693 570 08.
E-mail address: yujn@iris.ciae.ac.cn (J. Yu).

0022-3115/$ - see front matter © 2004 Elsevier B.V. All rights reserved.
doi:10.1016/j.jnucmat.2004.04.300

by JAERI to be used in a temperature range 250–450 °C and other DEMO designs may endanger the safety of FW and blanket system, especially a blanket concept cooled by pressurized water.

The dose dependence of impact properties for different advanced ferritic/martensitic alloys at low irradiation temperature seems to be in the low-dose range and is mainly an effect of helium generated by different levels of boron [8]. A complementary investigator [9] indicated that DBTT-shift (ΔDBTT) increases with helium content at 250 °C at doses up to 0.2 dpa. It is important to investigate the microstructure evolution under irradiation at low temperature with helium production rate at a fusion reactor level and address the low-temperature irradiation embrittlement. The TEM observation in F82H irradiated in three ways (590 MeV proton, 590 MeV proton + neutron, neutron) from 0.5 to 10 dpa at 250–310 °C with different helium levels indicated that there were no observable cavities, even at the highest studied dose [10].

In this paper, both low-temperature irradiation and helium effects on microstructure evolution of reduced activation martensitic steel EUROFER97 by dual beam irradiation with 10 He appm/dpa rate from 0–50 dpa were investigated and the helium and defects relative to the low-temperature irradiation embrittlement were addressed.

2. Experimental procedure

Specimens of EUROFER97, containing (in wt%) 8.9 chromium, 0.12 carbon, 0.46 manganese, 1.07 tungsten, 0.2 vanadium, 0.15 tantalum and iron for balance were used. The steel was conducted heat-treated by normalizing at 1253 K for 30 min and was fully martensitic after quenching. The tempering was conducted at 1033 K for 1.5 h. The prior austenite grain size was about 10 (ASTM). The specimens were punched out with 0.15 mm thickness and 3 mm diameter from a strip, which was cut from a thick plate of EUROFER97 with a wire cutting machine and milled to 0.15 mm thick. The disk specimens for TEM observation were electro-jet polished.

Dual-beam irradiations were conducted on a high voltage electron microscope (H-1300) and a 300 keV ion accelerator. The damage rate was 2×10^{-3} dpa/s, the irradiation dose varied from 0 to 50 dpa, and irradiation temperature was at 250 and 300 °C. The energy of helium ions was 100 keV and the injection rate was 10 appm/dpa, which corresponds to the helium production rate of fusion reactors. The damage caused by helium injection was less than 1% of that caused by electron irradiation, and thus can be neglected. The thickness of irradiated area was 400 nm as measured by thickness fringes. The electron beam diameter was 2.4 μm and the central diameter of the irradiated area was 1 μm. Electron beam was perpendicular to the specimen and the tilt angle of helium beam was 45° to the specimen. A low index crystalline plane (1 1 1) was chosen for electron beam irradiation. The microstructure was observed in situ at various stages in the irradiation process.

3. Experimental results and discussion

In-situ microstructure observation shows that the visible bubbles were present after 1.7 dpa for 250 °C irradiation and after 0.1 dpa for 300 °C irradiation. The images of the same region of the specimen irradiated at 250 °C from 1.7 to 50 dpa, shown in Fig. 1, indicate that bubbles evolve from tiny visible size to apparently large cavities. The bubble mean size and concentration in-

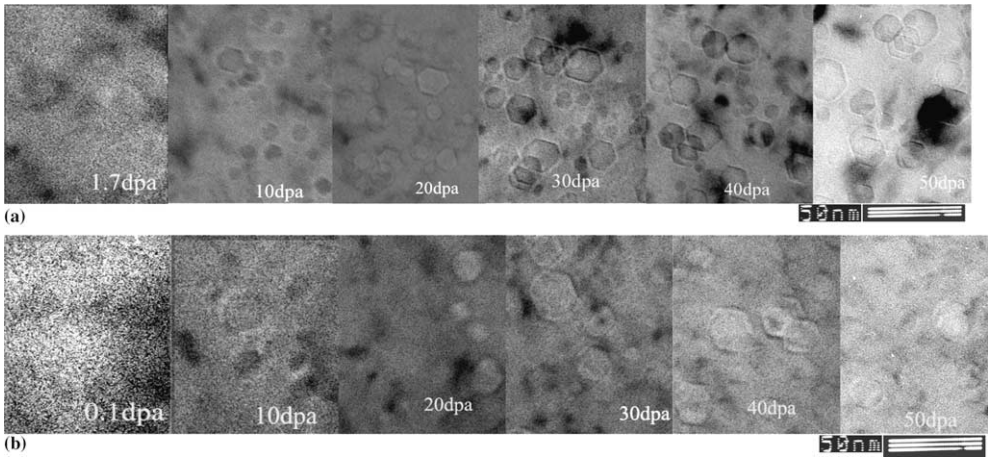

Fig. 1. Microstructure of EUROFER97 specimens irradiated by dual beams from 0.1 to 50 dpa with a helium production rate of 10 He appm/dpa at 250 °C (a) and 300 °C (b).

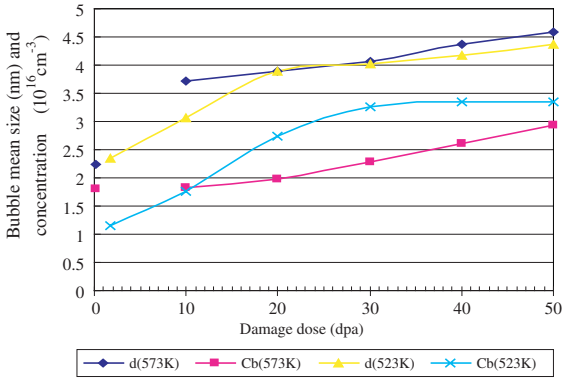

Fig. 2. Mean size (d) and concentration of bubbles (C_b, including cavities) with damage dose (dpa) at 250 and 300 °C irradiation.

crease with damage doses, shown in Fig. 2. The bubble size and concentration increase from 1.7 to 10 dpa. 'After 30 dpa the concentration increases slowly and approaches saturation at 50 dpa. The mean size and concentration range are similar to that observed by Schaublin and Victoria [10], but the present results obviously show bubbles and cavities, as well as interstitial dislocation loops.

The images of specimens irradiated at 300 °C are also shown in Fig. 1. The situation about bubble evolution from 0.1 to 50 dpa is similar to that at 250 °C. The bubble size of specimen irradiated at 300 °C is larger than that for irradiation at 250 °C; but the concentration for doses less than 10 dpa is higher than that for irradiation at 250 °C. For doses greater than 20 dpa, the concentration is lower. Lower temperatures cause higher nucleation rates. Therefore the bubble density is higher and bubble size is lower at lower temperature. Because of higher density of nuclei and lower growth rates at lower temperature, some bubble sizes are less than 1 nm before 10 dpa. These invisible bubbles are missing in account of bubble number. Therefore the bubble density at 250 °C before 10 dpa is lower than that for 300 °C irradiation. In addition the bubbles growth rate is higher at high irradiation temperature, the bubble size increases larger and the concentration becomes lower.

The swelling values after 50 dpa at 250 and 300 °C irradiation are 0.367×10^{-3} and 1.492×10^{-3}, respectively.

The bubble size distribution in the specimen irradiated at 250 °C from 1.7 to 50 dpa is shown in Fig. 3. The bubble size distribution at 1.7 dpa is similar to a Maxwell distribution and the peak is located around 2 nm. This suggests homogeneous bubble nucleation. As the dose increases, the bubble size distribution spreads out and the peak position shifts to a larger bubble size. After 30 dpa the bubble size distribution becomes bimodal; the first peak is around 2.5 nm and that of the second peak is around 6 nm. The bubble size and concentration of the first peak are similar values for various damage doses, but the bubble size distribution varies either a single peak or bimodal. The first peak is due to homogeneous bubble nucleation and growth, which remains throughout the whole irradiation process. Although the bubbles evolve to large bubble and cavities continuously, and at the same time the bubble nucleation and growth under dual-beam irradiation still complement the loss of bubbles which are evolving cavities. Therefore the bubble size and concentration of the first peak are around similar values for all the damage doses, and the number of cavities increases continuously. The second peak belongs to the cavity growth and spreads out with increasing

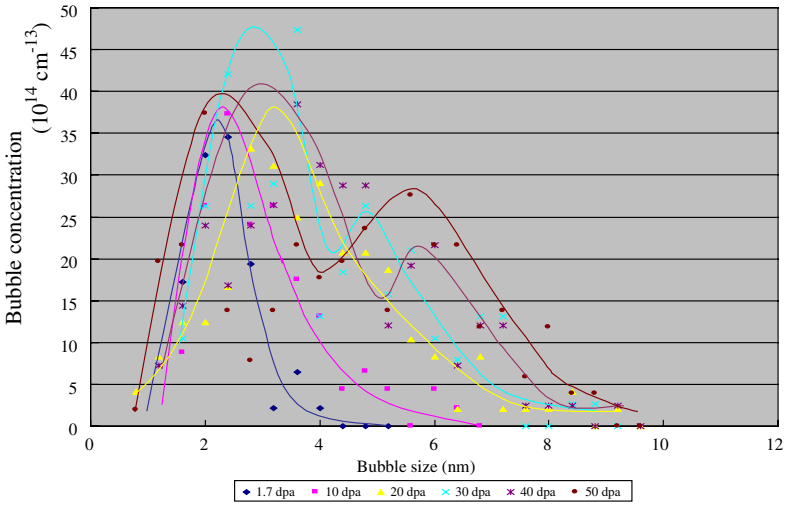

Fig. 3. Bubble (including cavity) size distribution for various damage doses at 250 °C irradiation.

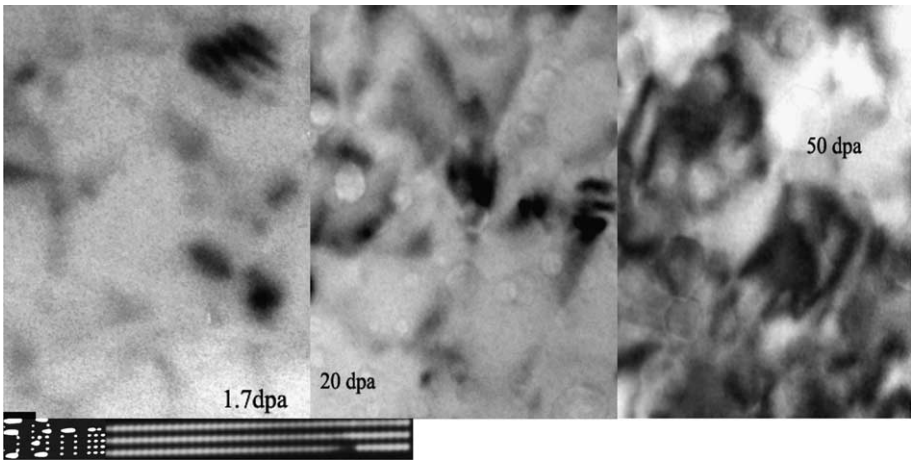

Fig. 4. Images of interstitial dislocation loops in specimen irradiated at 250 °C.

damage dose. Because the irradiation experiments with dual-beam irradiation in HVEM (H-1300 keV) were conducted step by step as the damage dose increased, the in-situ microstructure observations were at the plateau of the step without the dual-beam irradiation. After observation the surviving defects are sinks for vacancies and helium, and their growth will be faster during the next dual-beam irradiation. These will be deviating from the homogeneous nucleation and growth of the bubbles and cavities. Therefore the bubble size distribution spreads out and moves to larger bubble sizes.

The bubble size distribution of the specimen irradiated at 300 °C from 0.1 to 50 dpa is similar to that at 250 °C; the bubble evolution process is faster than that for irradiation at 250 °C and the bimodal distribution appeared at 10 dpa. Due to an increase in irradiation temperature, the bubble growth rate increases and the bubble size of the first peak shifts to large size with increasing damage dose.

The observation of dislocations in the specimens irradiated at 250 and 300 °C indicates that the dislocation loops are continuously produced by irradiation, which is typical interstitial dislocation loop. They evolve from black–white spots to visible interstitial loops. Fig. 4 shows the images of specimens irradiated to 1.7, 20, 50 dpa at 250 °C. The size range of interstitial loops is between 2.5 and 11 nm. There are no large dislocation loops whose size is larger than 11 nm, but the dislocation loop density continuously increases with the damage dose. The dense interstitial loop with small size will induce the increase of strength and the loss of ductility.

4. Summary

1. Bubbles and cavities are produced in the reduced activation martensitic steel EUROFER 97 under dual-beam irradiation with a helium rate of 10 He appm/dpa at 250 and 300 °C. The cavities result from bubble evolution. The swelling values at 50 dpa are 0.367×10^{-3} and 1.492×10^{-3} for irradiation temperatures of 250 and 300 °C, respectively. The bubble size is larger and the concentration is lower at the higher irradiation temperature.
2. The bubble and cavity size distribution progressively evolves from single Maxwell distribution to bimodal distribution. The concentration and size of bubbles at the first peak are similar for all damage doses. The cavity size distribution progressively develops to induce the second peak. The size of cavities at the second peak is around the 6 nm, but the cavity concentration in the second peak increases with damage dose and the distribution spreads out with increasing dose.
3. The dislocation loops are continuously produced by irradiation, which are typical interstitial dislocation loops and evolve from black–white spots to visible interstitial loops. The size range of interstitial loops is between 2.5 and 11 nm and the dislocation loop density monotonically increases with dose. The dense interstitial loop with small size will induce the increase of strength and the loss of ductility.

Acknowledgements

This work is support by CUP program and partly supported by Chinese National Natural Science Foundation with Grant No. 10375067.

References

[1] D.L. Smith, R.F. Mattas, M.C. Billone, in: R.W. Cahn, P. Haasen, E.J. Kramer (Eds.), Materials Science and Technology, vol. 10B, VCH, 1994, p. 257.

[2] B. van der Schaaf, D.S. Gelles, et al., J. Nucl. Mater. 283–287 (2000) 52.
[3] R.L. Klueh, D.S. Gelles, et al., J. Nucl. Mater. 307–312 (2002) 455.
[4] T. Muroga, M. Gasparotto, S.J. Zinkle, Fus. Eng. Des. 61&62 (2002) 13.
[5] T. Hasegawa, Y. Tomita, et al., J. Nucl. Mater. 258–263 (1998) 1153.
[6] J.G. van der Lann et al., Fus. Eng. Des., in press.
[7] K. Shiba, A. Hishinuma, J. Nucl. Mater. 283–287 (2000) 474.
[8] M. Rieth, B. Daffenrner, H.D. Rohrig, J. Nucl. Mater. 258–263 (1998) 1147.
[9] R. Lindau, A. Moslang, D. Preininger, et al., J. Nucl. Mater. 271&272 (1999) 450.
[10] R. Schaublin, M. Victoria, J. Nucl. Mater. 283–287 (2003) 339.